

Ion Acoustic Waves in Ultracold Neutral Plasmas

J. Castro, P. McQuillen, and T.C. Killian

Rice University, Department of Physics and Astronomy and Rice Quantum Institute, Houston, Texas 77005.

(Dated: May 26, 2010)

We photoionize laser-cooled atoms with a laser beam possessing spatially periodic intensity modulations to create ultracold neutral plasmas with controlled density perturbations. Laser-induced fluorescence imaging reveals that the density perturbations oscillate in space and time, and the dispersion relation of the oscillations matches that of ion acoustic waves, which are long-wavelength, electrostatic, density waves.

Collective wave phenomena are central to the transport and thermodynamic properties of plasmas, and the presence of a rich spectrum of collective modes is a distinctive feature that separates this state of matter from a simple collection of charged particles [1]. In ultracold neutral plasmas (UNPs) [2, 3], which are orders of magnitude colder than any other neutral plasma and can be used to explore the physics of strongly coupled systems [4–6], little work has been done to study collective modes [7–10]. Here we employ a new technique for creating controlled density perturbations to excite ion acoustic waves (IAWs) in an UNP and measure their dispersion relation. This flexible technique for sculpting the density distribution will open new areas of plasma dynamics for experimental study, including the effects of strong coupling on dispersion relations [11–14] and non-linear phenomena [3, 10, 15, 16] in the ultracold regime.

UNPs are formed by photoionizing laser-cooled atoms near the ionization threshold. They stretch the boundaries of traditional neutral plasma physics and have extremely clean and controllable initial conditions that make them ideal for studying phenomena seen in more complex systems, such as plasma expansion and equilibration in high-energy-density laser-matter interactions [5] and quark-gluon plasmas [6]. UNPs have shown fascinating dynamics, such as kinetic energy oscillations that directly reflect the strong coupling of ions [5, 17]. Strong coupling arises when particle interaction energies exceed the kinetic energy [4]. It is important in many fields of physics spanning classical to quantum behavior [5, 6, 18, 19] and gives rise to phase transitions and the establishment of spatial correlations of particles [4]. These studies complement experiments probing strong coupling in dusty plasmas [18] and non-neutral plasmas of pure ions or electrons [19].

Previous experimental studies of collective modes in UNPs were limited to excitations of Langmuir (electron density) oscillations with radio frequency electric fields [7, 8] which did not determine a dispersion relation and were relatively insensitive to dynamics of the strongly coupled ions. A high-frequency electron drift instability was observed in an UNP in the presence of crossed electric and magnetic fields [9]. Spherically symmetric ion density modulations were shown to excite IAWs in numerical simulations of UNPs [10]. Here we excite IAWs through direct imprinting of ion density modulations dur-

ing plasma formation and image them in situ with time resolved laser-induced fluorescence [20].

Low frequency electrostatic, or longitudinal ion density waves are one of the most fundamental oscillations in a plasma along with Langmuir oscillations [21]. A hydrodynamic plasma description, assuming slow enough ion motion for electrons to remain isothermal and an infinite homogeneous medium, predicts the dispersion relation for frequency ω and wavevector k [1]

$$\left(\frac{\omega}{k}\right)^2 = \frac{k_B T_e / M}{1 + k^2 \lambda_D^2} \quad (1)$$

where M is the ion mass, T_e is electron temperature, and $\lambda_D \equiv \sqrt{\epsilon_0 T_e / n_e e^2}$ is the Debye screening length, for electron density n_e and proton charge e . We have neglected an ion pressure term because the ion temperature satisfies $T_i \ll T_e$ in UNPs. In the long wavelength limit, which is the focus of this study, this mode takes the form of an IAW with $\omega = k \sqrt{k_B T_e / M}$, in which ions provide the inertia and electrons provide the restoring pressure.

IAWs are highly Landau damped unless $T_i \ll T_e$ [1], however, they have been studied in many types of high-temperature laboratory plasmas [15, 16, 22]. Closely related to this work, acoustic waves of highly charged dust particles in dusty plasmas have been studied experimentally [23, 24] and theoretically [11–14] because of the possibility of observing the effects of strong coupling on the dispersion relation, but to date these effects have been masked by damping due to collisions with background neutral gas [11, 13, 25]. Beyond fundamental interest, IAWs are invoked to explain wave characteristics observed in Earth's ionosphere [26] and transport in the solar wind, corona, and chromosphere [27].

UNPs are created through photoionization of laser-cooled strontium atoms from a magneto-optical trap (MOT) [3]. The MOT operates on the $^{88}\text{Sr } ^1\text{S}_0 - ^1\text{P}_1$ resonance at 461 nm [30], trapping $\sim 3 \times 10^8$ atoms at ~ 10 mK with a spherical Gaussian density distribution. Photoionization is a two-photon process: the first from a pulse amplified laser beam operating on the Sr trapping transition, and the second from a 10 ns Nd:YAG pumped dye laser tunable around 412 nm [3]. This process ionizes $\sim 50\%$ of the atoms, and the plasma inherits its density distribution from the neutral atoms. Effects of un-ionized atoms on the plasma are not observed because of the fast time-scales of the experiment and small

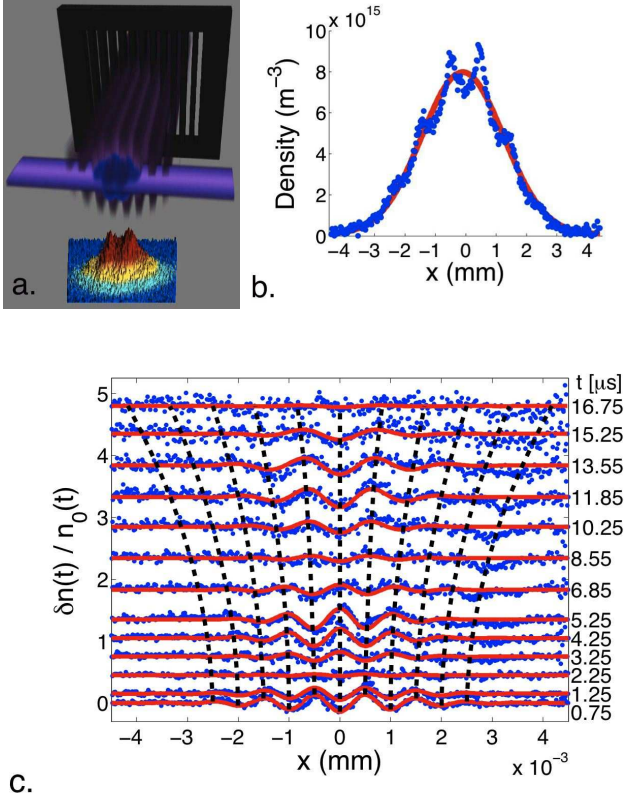


FIG. 1: Excitation, imaging and modeling of density perturbations in an UNP. a, A periodic transmission mask modulates the ionization beam intensity to excite IAWs. An adjustable delay later, a sheet of laser light near resonant with the principle transition in the ions, illuminates a central slice of plasma, and laser-induced fluorescence along a perpendicular direction is captured by an imaging system to form a two-dimensional false color plot of the ion density distribution. b, 1D slice through the density profile for $T_e(0) = 105$ K and 1 mm mask period, 750 ns after ionization. Deviations from the fit Gaussian represent the IAW density modulation, δn . c, Evolution of δn for the same initial conditions as figure 1b. Time since ionization is indicated on the right, and δn has been scaled by instantaneous peak density $n_0(t)$ and offset for clarity. Solid red lines are fits to equation (4), and the dotted black lines follow the wave nodes and antinodes with time.

neutral-ion collision cross-sections.

Resulting electron temperatures are determined by the excess energy of the ionizing photons above threshold, and are adjustable from 1-1000 K. Ion temperatures of approximately 1 K are set by disorder-induced heating [17, 28, 29] during the thermalization of the ions, and result in strongly-coupled ions in the liquid-like regime [3, 4]. Density distributions are spherical Gaussians, $n(r) = n_0 \exp(-r^2/2\sigma_0^2)$, with $n_0 \sim 10^{15} \text{ cm}^{-3}$ and $\sigma_0 \sim 1.5 \text{ mm}$, yielding average λ_D from 3-30 μm . In our experiments, no magnetic field is applied.

IAWs were excited by passing the 412 nm ionizing beam, after its first pass through the plasma, through a periodic transmission mask and retroreflecting it back onto the plasma. This creates a $\sim 10\%$ plasma density modulation with wavelength set by the period (λ_0) of the mask (Fig. 1a). The mask pattern is translated to align a density minimum to the center of the plasma. Small higher-harmonic IAWs, arising from the square-wave nature of the mask, were observed for longer period gratings, but no effect on the fundamental wave was detected.

For a diagnostic, ions are optically excited on the primary Sr^+ transition, $^2\text{S}_{1/2} - ^1\text{P}_{1/2}$, with a tuneable, narrowband (~ 5 MHz) laser at $\lambda = 422$ nm, propagating approximately perpendicular to the ionizing laser [3, 20]. The 422 nm beam is masked with a 1 mm slit so it only illuminates a central slice of the plasma, and resulting laser-induced fluorescence emitted close to perpendicular to the plane of the ionizing and 422 nm beams is imaged onto an intensified CCD camera with a resolution of 13 μm .

Data from ~ 50 repetitions of the experiment is summed to form a single image, $F(x, y, \nu)$, that has a frequency (ν) dependence reflecting the natural linewidth and Doppler-broadening of the transition [3, 20]. 40 images are recorded at evenly-spaced frequencies for the 422 nm laser spanning the full spectral width of the signal. These are summed to obtain a signal proportional to the density of the plasma in the illuminated plane ($z \approx 0$),

$$\sum_{\nu} F(x, y, \nu) \propto n_i(x, y, z \approx 0). \quad (2)$$

Density averaging along the imaging axis (z) is small because fluorescence is only excited in a sheet of plasma. Absolute determination of density is obtained by calibrating fluorescence signals against absorption images of the plasma [3, 20].

Figure 1b shows a central 1D slice through density data along the modulation direction. The difference between a fit Gaussian distribution and the data yields the density perturbation δn as shown in Fig. 1c. Note the oscillation of the wave in time and the changing wavelength of the excitation.

The perturbation has a negligible effect on the global dynamics of the plasma, which is dominated by expansion into the surrounding vacuum. For an initial Gaussian density distribution and conditions such as used here in which inelastic electron-ion collisions are negligible, the expansion is self-similar and the characteristic plasma size changes according to [3]

$$\sigma(t) = \sigma_0 (1 + t^2/\tau_{exp}^2)^{1/2}, \quad (3)$$

where $\tau_{exp} \approx \sqrt{M\sigma_0^2/k_B T_e(0)}$ is the characteristic plasma expansion time, which ranges from 10-30 μs in this study. Associated with expansion is an adiabatic cooling of electrons according to $T_e(t) = T_e(0)/(1 +$

t^2/τ_{exp}^2), which shows that expansion is driven by a transfer of electron thermal energy to the kinetic energy of ion expansion. In direct measurements of plasma size and spectral measurement of ion expansion velocity [20], we saw no deviation in expansion dynamics due to the presence of density modulations.

To describe wave data such as Fig. 1c, we scale the amplitude to the peak density at $t = 0$ of the Gaussian fit (Fig. 1b) and assume a damped standing wave with a Gaussian envelope,

$$\begin{aligned} \frac{\delta n}{n(0)} &= \frac{\delta n_0}{n(0)} e^{-x^2/2\sigma_{env}(t)^2} \cos[k(t)x] \cos[\phi(t)] e^{-\Gamma t} \\ &= A(t) e^{-x^2/2\sigma_{env}(t)^2} \cos[k(t)x]. \end{aligned} \quad (4)$$

This expression fits the modulation at a single time, t , and yields the instantaneous amplitude $A(t)$, envelope size $\sigma_{env}(t)$ and wavevector $k(t)$. The hydrodynamic description for an infinite homogeneous medium used to derive the IAW dispersion relation, Eq. 1, allows for planar standing-wave solutions, but finite size, plasma expansion, and density inhomogeneity introduce additional factors that are not small here and preclude an analytic solution, so this model is only phenomenological.

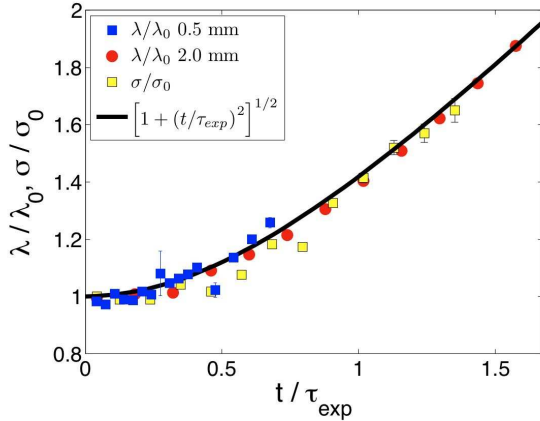


FIG. 2: Evolution of the IAW wavelength and plasma size, normalized to initial values, for $T_e(0) = 70$ K and $\sigma_0 = 1.45$ mm. Both quantities follow a universal curve indicating the wave vector expands with the plasma. For the solid line, τ_{exp} has been set to its theoretical value.

To examine the effect of the expanding plasma on the wave we compare the change in the wavelength with the changing size of the plasma by plotting, in Fig. 2, $\lambda(t)/\lambda_0 = k_0/k(t)$ and $\sigma(t)/\sigma_0$, where all quantities have been normalized to the values at $t = 0$. Initial wavelengths match the period of the mask used. All data follow one universal curve, $(1 + t^2/\tau_{exp}^2)^{1/2}$, with τ_{exp} corresponding to σ_0 and $T_e(0)$ as indicated in Eq. 3.

The agreement for the wavelength indicates the wave is pinned to the expanding density distribution.

To extract the frequency of the wave, $\omega(t)$, we fit the amplitude variation in time, accounting for the evolution of the phase, as

$$A(t) = A_0 e^{-\Gamma t} \cos[\phi(t)] = A_0 e^{-\Gamma t} \cos\left(\int_0^t \omega(t') dt'\right). \quad (5)$$

We assume the form of the dispersion for an infinite, homogeneous medium from Eq. 1, the observed variation of wave-vector $k(t)$, and electron temperature evolution $T_e(t)$ predicted for a self similar expansion [3] to obtain

$$\omega(t) = k(t) \sqrt{k_B T_e(t)/M} = \omega_0 \left(\frac{1}{1 + t^2/\tau_{exp}^2} \right). \quad (6)$$

Initial amplitude A_0 and frequency ω_0 , and damping rate Γ are allowed to vary in the fits, which match the data very well (Fig. 3). Decreasing frequency with time was observed in simulations of spherical IAWs [10].

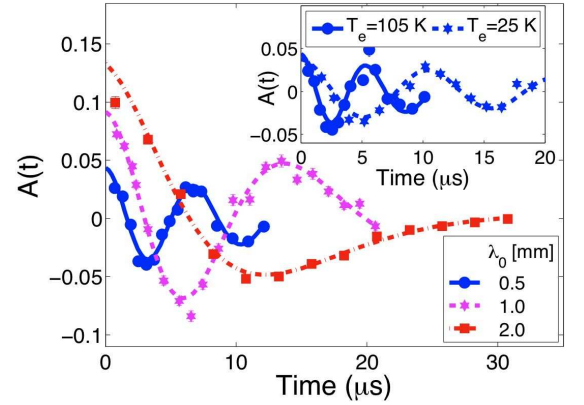


FIG. 3: Evolution of wave amplitude and fits to obtain $\omega(t)$. The main plot shows the instantaneous amplitude for various mask periods with $T_e(0) = 70$ K. The inset similarly compares data for different initial electron temperatures with $\lambda_0 = 0.50$ mm. Lines are fits to equation (5) in which τ_{exp} has been fixed to the theoretical value.

For a range of initial electron temperatures and mask periods, we extract ω_0 and k_0 and calculate the dispersion of the excitations, as shown in Fig. 4. The excellent agreement with theory, Eq. 1, confirms that these excitations are IAWs. The planar standing-wave model captures the dominant behaviour of the wave, and to a high accuracy there is no deviation from the standard dispersion relation in spite of the plasma's finite size, expansion, and inhomogeneous density.

Following on this initial study of ion density excitations in an UNP, there are many topics to explore. The

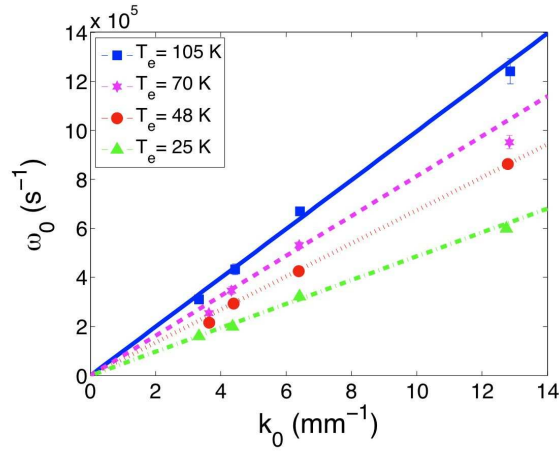


FIG. 4: Dispersion relation of IAWs for different initial electron temperatures. Lines are from the theoretical dispersion relation, Eq. 1, with no fit parameters.

observed waves show damping times on the order a few oscillation periods, which is faster than predicted for Landau damping [1]. The nature of the boundary conditions and effects of density inhomogeneity and plasma expansion on IAWs should be explored, and may be important for understanding damping. The mask period is currently limited by diffraction effects, but this can be overcome by modifying the optical configuration. For mask periods approximately five times smaller, we can probe beyond the acoustic region of the dispersion relation. In this regime, the effects of strong coupling on dispersion are also predicted to be important, and there are many theoretical predictions that have not been tested [11–14]. The wave can be studied in velocity space with resolved fluorescence spectroscopy [20], and different initial density distributions can be designed to investigate solitons [15], instabilities [16], asymmetric excitations, and shock waves [3, 10].

This work was supported by the David and Lucille Packard Foundation and the Department of Energy and National Science Foundation (PHY-0714603).

-
- [1] T. H. Stix, *Waves in Plasmas* (AIP, New York, 1992), 2nd ed.
 - [2] T. C. Killian, *Science* **316**, 705 (2007).
 - [3] T. C. Killian, T. Pattard, T. Pohl, and J. M. Rost, *Phys. Rep.* **449**, 77 (2007).
 - [4] S. Ichimaru, *Statistical Plasma Physics, Volume II: Condensed Plasmas*, vol. 2 of *Frontiers in Physics* (Westview Press, Boulder, CO, 2004).
 - [5] M. S. Murillo, *Phys. Rev. Lett.* **96**, 165001 (2006).
 - [6] S. Mrwczynski and M. H. Thoma, *Annu. Rev. Nuc. and Part. Sci.* **57**, 61 (2007).
 - [7] R. S. Fletcher, X. L. Zhang, and S. L. Rolston, *Phys. Rev. Lett.* **96**, 105003 (2006).
 - [8] S. Kulin, T. C. Killian, S. D. Bergeson, and S. L. Rolston, *Phys. Rev. Lett.* **85**, 318 (2000).
 - [9] X. L. Zhang, R. S. Fletcher, and S. L. Rolston, *Phys. Rev. Lett.* **101**, 195002 (2008).
 - [10] F. Robicheaux and J. D. Hanson, *Phys. Plasmas* **10**, 2217 (2003).
 - [11] M. Rosenberg and G. Kalman, *Phys. Rev. E* **56**, 7166 (1997).
 - [12] M. S. Murillo, *Phys. Plasmas* **5**, 3116 (1998).
 - [13] P. K. Kaw, *Phys. Plasmas* **8**, 1870 (2001).
 - [14] H. Ohta and S. Hamaguchi, *Phys. Rev. Lett.* **84**, 6026 (2000).
 - [15] Y. Nakamura, H. Bailung, and P. K. Shukla, *Phys. Rev. Lett.* **83**, 1602 (1999).
 - [16] M. Yamada and M. Raether, *Phys. Rev. Lett.* **32**, 99 (1974).
 - [17] Y. C. Chen, C. E. Simien, S. Laha, P. Gupta, Y. N. Martinez, P. G. Mickelson, S. B. Nagel, and T. C. Killian, *Phys. Rev. Lett.* **93**, 265003 (2004).
 - [18] G. E. Morfill and A. V. Ivlev, *Rev. Mod. Phys.* **81**, 1353 (2009).
 - [19] D. H. E. Dubin and T. M. O’Neil, *Rev. Mod. Phys.* **71**, 87 (1999).
 - [20] J. Castro, H. Gao and T. C. Killian, *Journal of Plasma Physics and Controlled Fusion* **50**, 124011 (2008).
 - [21] L. Tonks and I. Langmuir, *Phys. Rev.* **33**, 195 (1929).
 - [22] N. Rynn and N. D’Angelo, *Rev. Sci. Instrum.* **31**, 1326 (1960).
 - [23] A. Barkan, R. L. Merlino, and N. D’Angelo, *Phys. Plasmas* **2**, 3563 (1995).
 - [24] J. B. Pieper and J. Goree, *Phys. Rev. Lett.* **77**, 3137 (1996).
 - [25] X. Wang and A. Bhattacharjee, *Phys. Plasmas* **4**, 3759 (1997).
 - [26] M. E. Koepke, *Phys. Plasmas* **9**, 2420 (2002).
 - [27] S. R. Cranmer, A. A. van Ballegoijen, and R. J. Edgar, *Astrophys. J.* **171**, 520 (2007).
 - [28] M. S. Murillo, *Phys. Rev. Lett.* **87**, 115003 (2001).
 - [29] E. A. Cummings, J. E. Daily, D. S. Durfee, and S. D. Bergeson, *Phys. Rev. Lett.* **95**, 235001 (2005).
 - [30] S. B. Nagel, C. E. Simien, S. Laha, P. Gupta, V. S. Ashoka, and T. C. Killian, *Phys. Rev. A* **67**, 011401(R) (2003).